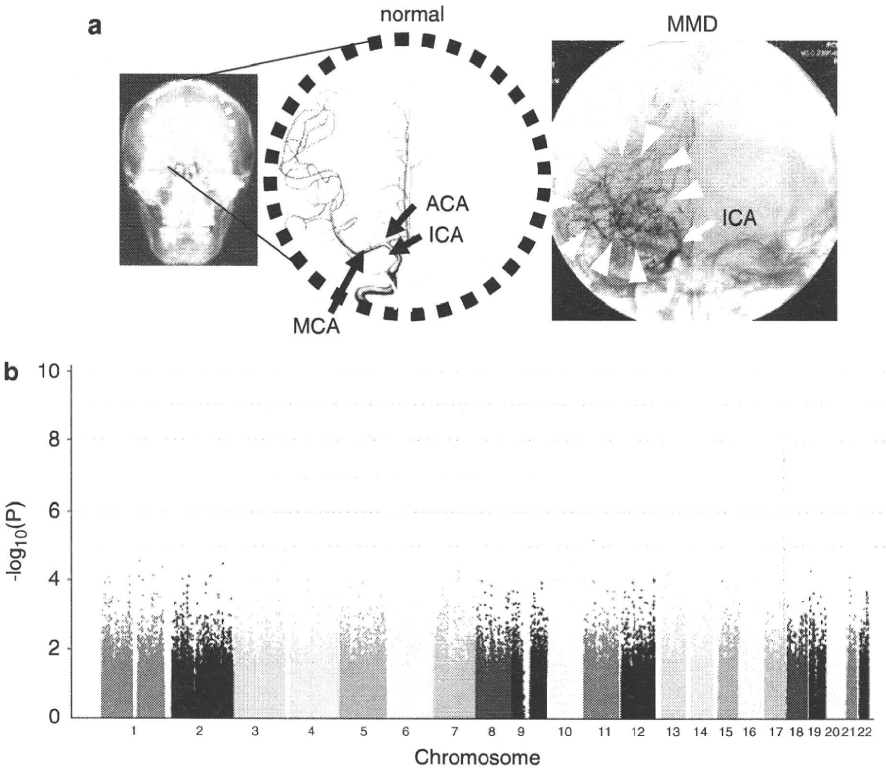

Figure 1 (**a**) Abnormal brain vessels in MMD. The dotted circle indicates the X-ray field of cerebral angiography (left panel). Normal structures of the right internal carotid artery (ICA), anterior cerebral artery (ACA) and middle cerebral artery (MCA) are illustrated (middle panel). The arrowheads indicate abnormal collateral vessels appearing like a puff of smoke in the angiogram of an individual with MMD (right panel). Note that ACA and MCA are barely visible, because of the occlusion of the terminal portion of the ICA. (**b**) Manhattan plot of the 785 720 SNPs used in the genome-wide association analysis of MMD patients. Note that the SNPs in the 17q25-ter region reach a significance of $P < 10^{-8}$.

MATERIALS AND METHODS

Affected individuals

Genomic DNA was extracted from blood and/or saliva samples obtained from members of the families with MMD (Supplementary Figure 1), MMD patients with no family history and control subjects. All of the subjects were Japanese. MMD was diagnosed on the basis of guidelines established by the Research Committee on Spontaneous Occlusion of the Circle of Willis of the Ministry of Health and Welfare of Japan. This study was approved by the Ethics Committee of Tohoku University School of Medicine. Total RNA samples were purified from leukocytes using an RNeasy mini kit (Qiagen, Hilden, Germany) and used as templates for cDNA synthesis with an Oligo $(dT)_{20}$ primer and SuperScript II reverse transcriptase according to the manufacturer's instructions (Invitrogen, Carlsbad, CA, USA).

Linkage analysis

For the linkage analysis, DNA samples were genotyped for 36 microsatellite markers within five previously reported MMD loci using the ABI 373A DNA Sequencer (Applied Biosystems, Foster City, CA, USA). Pedigrees and haplotypes were constructed with the Cyrillic version 2.1 software (Oxfordshire, UK). Multipoint analyses were conducted using the GENEHUNTER 2 software (http://www.broadinstitute.org/ftp/distribution/software/genehunter/). Statistical analysis was performed with SPSS version 14.0J (SPSS, Tokyo, Japan).

Genome-wide and locus-specific association studies

A genome-wide association study was performed using a group of 72 MMD patients, which consisted of 64 patients without a family history of MMD and 8 probands of MMD families. The Illumina Human Omni-Quad 1 chip (Illumina, San Diego, CA, USA) was used for genotyping, and single-nucleotide polymorphisms (SNPs) with a genotyping completion rate of 100% were used for further statistical analysis (785 720 out of 1 140 419 SNPs). Genotyping data from 45 healthy Japanese controls were obtained from the database at the International HapMap Project web site. The 785 720 SNPs were statistically analyzed using the PLINK software (http://pngu.mgh.harvard.edu/~purcell/plink/index.shtml). For a locus-specific association study, we used 63 DNA samples consisting of 58 non-familial MMD patients and 5 probands of MMD families. A total of 384 SNPs within chromosome 17q25-ter were genotyped (Supplementary Table 1), using the GoldenGate Assay and a custom SNP chip (Illumina). Genotyping data for 45 healthy Japanese were used as a control. Case–control single-marker analysis, haplotype frequency estimation and significance testing of differences in haplotype frequency were performed using the Haploview version 3.32 program (http://www.broad.mit.edu/mpg/haploview/).

Mutation detection

Mutational analyses of *RNF213* and *FLJ35220* were performed by PCR amplification of each coding exon and putative promoter regions, followed by direct sequencing. Genomic sequence data for the two genes were obtained from the National Center for Biotechnology Information web site (http://www.ncbi.nlm.nih.gov/) for design of exon-specific PCR primers. *RNF213* cDNA fragments were amplified from leukocyte mRNA for sequencing analysis. Sequencing of the PCR products was performed with the ABI BigDye Terminator Cycle Sequencing Reaction Kit using the ABI 310 Genetic Analyzer. Identified base changes were screened in control subjects. Statistical difference of the carrier frequency of each base change was estimated by Fisher's exact test (the MMD group vs the control group).

Quantitative PCR

MTC Multiple Tissue cDNA Panels (Clontech Laboratory, Madison, WI, USA) were the source of cDNAs from human cell lines, adult and fetal tissues. Mononuclear cells and polymorphonuclear cells were isolated from the fresh peripheral blood of healthy human adults using Polymorphprep (Cosmo Bio,

Carlsbad, CA, USA). T and B cells were isolated from the fresh peripheral blood of healthy human adults using the autoMACS separator (Militeny Biotec, Bergisch Gladbach, Germany). Total RNA was isolated from these cells with the RNeasy Mini Kit (Qiagen) following the manufacturer's instructions. We reverse transcribed 100 ng samples of total RNA into cDNAs using the High Capacity cDNA Reverse Transcription Kit (Applied Biosystems). Quantitative PCRs were performed in a final volume of 20 µl using the FastStart TaqMan Probe Master (Rox) (Roche, Madison, WI, USA), 5 µl of cDNA, 10 µM of *RNF*- or *GAPDH*-specific primers and 10 µM of probes (Universal ProbeLibrary Probe #80 for *RNF213* and Roche Probe #60 for *GAPDH*). All reactions were performed in triplicate using the ABI 7500 Real-Time PCR system (Applied Biosystems). Cycling conditions were 2 min at 50°C and 10 min at 95°C, followed by 40 cycles of 15 s at 95°C and 60 s at 60°C. Real-time PCR data were analyzed by the SDS version 1.2.1 software (Applied Biosystems). We evaluated the relative level of *RNF213* mRNA by determining the C_T value, the PCR cycle at which the reporter fluorescence exceeded the signal baseline. *GAPDH* mRNA was used as an internal reference for normalization of the quantitative expression values.

Multiplex PCR

MTC Multiple Tissue cDNA Panels (Clontech) were the source of human cell lines and cDNAs from human adult and fetal tissues. Multiplex PCRs were performed in a final volume of 20 µl using the Multiplex PCR Master Mix (Qiagen), 2 µl of cDNA, a 2 µM concentration of *RNF213* and a 10 µM concentration of *GAPDH*-specific primers. The samples were separated on a 2% agarose gel stained with ethidium bromide. Cycling conditions were 15 min at 94°C, followed by 30 cycles of 30 s at 94 °C, 30 s at 57 °C and 30 s at 72 °C. For normalization of the expression levels, we used *GAPDH* as an internal reference for each sample.

In situ hybridization (ISH) analysis

Paraffin-embedded blocks and sections of mouse tissues for ISH were obtained from Genostaff (Tokyo, Japan). The mouse tissues were dissected, fixed with Tissue Fixative (Genostaff), embedded in paraffin by proprietary procedures (Genostaff) and sectioned at 6 µm. To generate anti-sense and sense RNA probes, a 521-bp DNA fragment corresponding to nucleotide positions 470–990 of mouse *Rnf213* (BC038025) was subcloned into the pGEM-T Easy vector (Promega, Madison, WI, USA). Hybridization was performed with digoxigenin-labeled RNA probes at concentrations of 300 ng ml^{-1} in Probe Diluent-1 (Genostaff) at 60 °C for 16 h. Coloring reactions were performed with NBT/BCIP solution (Sigma-Aldrich, St Louis, MO, USA). The sections were counterstained with Kernechtrot stain solution (Mutoh, Tokyo, Japan), dehydrated and mounted with Malinol (Mutoh). For observation of *Rnf213* expression in activated lymphocytes, 10-week-old Balb/c mice were intraperitoneally injected with 100 µg of keyhole limpet hemocyanin and incomplete adjuvant and sacrificed in 2 weeks. The spleen of the mice was removed for Hematoxylin–eosin staining and ISH analyses.

RESULTS

Using 20 Japanese MMD families, we reevaluated the linkage mapped previously to five putative MMD loci. No locus with significant linkage, Lod score >3.0 or NPL score >4.0 was confirmed (Supplementary Figure 2). We conducted a genome-wide association study of 72 Japanese MMD cases. Single-marker allelic tests comparing the 72 MMD cases and 45 controls were performed for 785 720 SNPs using χ^2 statistics. These tests identified a single locus with a strong association with MMD ($P<10^{-8}$) on chromosome 17q25-ter (Figure 1b), which is in line with the latest mapping data of a MMD locus.[16] The SNP markers with $P<10^{-6}$ are listed in Table 1. To confirm this observation, we performed a locus-specific association study. A total of 384 SNP markers (Supplementary Table 1) were selected within the chromosome 17q25-ter region and genotyped in a set of 63 MMD cases and 45 controls. The SNP markers demonstrating a high association with MMD ($P<10^{-6}$) were clustered in a 151-kb region from base position 75 851 399–76 003 020 (SNP No.116–136 in

Table 1 A genome-wide association study of Japanese MMD patients and controls

	SNP	Chromosome	Base position	Gene	Risk allele/ non-risk allele	Risk allele frequency in MMD	Risk allele frequency in controls	χ^2	P-value	Odds ratio	95% confidence interval	
											Lower	Upper
1	rs11870849	17	76 025 668	*RNF213*	T/C	0.4792	0.1111	33.55	6.95E-09	7.36	3.532	15.34
2	rs6565681	17	75 963 089	*RNF213*	A/G	0.7361	0.3667	31.35	2.16E-08	4.819	2.733	8.489
3	rs7216493	17	75 941 953	*RNF213*	G/A	0.75	0.3889	30.39	3.53E-08	4.715	2.673	8.313
4	rs7217421	17	75 850 055	*RNF213*	A/G	0.6667	0.3	29.86	4.64E-08	4.666	2.642	8.237
5	rs12449863	17	75 857 806	*RNF213*	C/T	0.6667	0.3	29.86	4.64E-08	4.666	2.642	8.237
6	rs4890009	17	75 926 103	*RNF213*	G/A	0.8819	0.5778	28.5	9.38E-08	5.459	2.831	10.527
7	SNP17-75933731	17	75 933 731	*RNF213*	G/A	0.8819	0.5778	28.5	9.38E-08	5.458	2.831	10.527
8	rs7219131	17	75 867 365	*RNF213*	T/C	0.6667	0.3111	28.11	1.15E-07	4.429	2.517	7.794
9	rs6565677	17	75 932 037	*RNF213*	T/C	0.7431	0.3977	27.43	1.63E-07	4.378	2.483	7.722
10	rs4889848	17	75 969 256	*RNF213*	C/T	0.75	0.4111	26.99	2.05E-07	4.297	2.444	7.889
11	rs7224239	17	75 969 771	*RNF213*	A/G	0.8681	0.5667	26.99	2.05E-07	5.03	2.659	9.529

Abbreviations: MMD, moyamoya disease; SNP, single-nucleotide polymorphism.A genome-wide association study testing 1 140 419 SNPs on the Human Omni-Quad 1chip (Illumina, San Diego, CA, USA) was performed in 72 Japanese MMD cases. Single-marker allelic tests between the cases and controls were performed using χ^2 statistics for all markers. This table lists the 11 SNP markers with a significance of $P<10^{-6}$.

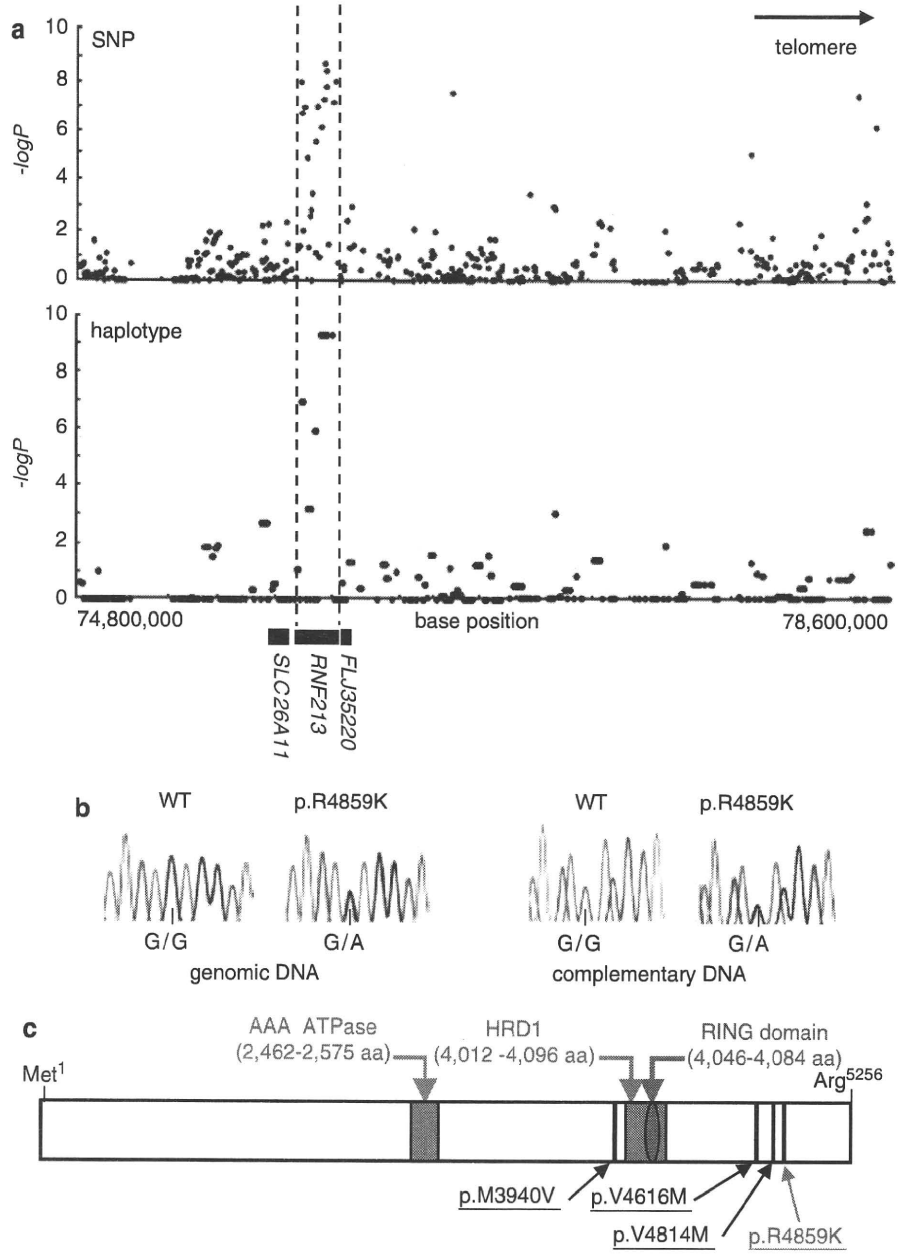

Figure 2 (**a**) Association analysis of 63 non-familial MMD cases and 45 control subjects. Statistical significance was evaluated by the χ^2-test. SNP markers with a strong association with MMD ($P<10^{-6}$) clustered in a 161-kb region (base position 75 851 399–76 012 838) indicated by two dotted lines (upper panel), which included the entire region of *RNF213* (lower panel). Haplotype analysis revealed a strong association ($P=5.3\times10^{-10}$) between MMD and a single haplotype located within *RNF213*. (**b**) Sequencing chromatograms of the identified MMD mutations. The left panel shows the sequences of an unaffected individual and a carrier of a p.R4859K heterozygous mutation. The right panel indicates the sequencing chromatograms of the leukocyte cDNA obtained from an unaffected individual and an individual with MMD who carries the p.R4859K mutation. Note that both wild-type and mutant alleles were expressed in leukocytes. (**c**) The structure of the RNF213 protein. The RNF213 protein contains three characteristic structures, the AAA-superfamily ATPase motif, the RING motif and the HMG-CoA reductase degradation motif. The positions of four mutations identified in MMD patients are underlined, including one prevalent mutation (red) and three private mutations (black).

Supplementary Table 1); this entire region was within the *RNF213* locus (Figure 2a). A single haplotype determined by seven SNPs (SNP Nos.130–136 in Supplementary Table 1) that resided in the 3′ region of *RNF213* was strongly associated with MMD onset ($P=5.3\times10^{-10}$). Analysis of the linkage disequilibrium block indicated that this haplotype was not in complete linkage disequilibrium with any other haplotype in this region (Supplementary Figure 3). These results strongly suggest that a founder mutation may exist in the 3′ part of *RNF213*.

Mutational analysis of the entire coding and promoter regions of *RNF213* and *FLJ35220*, a gene 3′ adjacent to *RNF213*, revealed that 19 of the 20 MMD families shared the same single base substitution, c.14576G>A, in exon 60 of *RNF213* (Figure 2b and Table 2). This nucleotide change causes an amino-acid substitution from arginine^{4859} to lysine^{4859} (p.R4859K). The p.R4859K mutation was identified in 46 of 63 non-familial MMD cases (73%), including 45 heterozygotes and a single homozygote (Table 3). Both the wild-type and the p.R4859K mutant alleles were co-expressed in leukocytes

Table 2 Nucleotide changes with amino-acid substitutions identified in the sequencing analysis of *RNF213* and *FLJ35220*

			Genotype (allele)				
Gene	*Exon*	*Nucleotide change[a] (amino-acid substitution)*	*Non-familial cases*	*Control subjects*	*P-value[b]*	*χ^2 (df=1)[c]*	*Odds ratio (95% CI)*
RNF213	29	c.7809C>A (p.D2603E)	2/63 (2/126)	15/381 (15/762)	0.77	0.09	0.80 (0.2–3.6)
RNF213	41	c.11818A>G (p.M3940V)	1/63 (1/126)	0/388 (0/776)	0.01	6.17	ND
RNF213	41	c.11891A>G (p.E3964G)	4/63 (4/126)	3/55 (4/110)	0.84	0.04	1.2 (0.3–5.5)
RNF213	52	c.13342G>A (p.A4448T)	4/63 (4/126)	2/53 (2/106)	0.53	0.39	1.7 (0.3–9.8)
RNF213	56	c.13846G>A (p.V4616M)	1/63 (1/126)	0/388 (0/776)	0.01	6.17	ND
RNF213	59	c.14440G>A (p.V4814M)	1/63 (1/126)	0/388 (0/776)	0.01	6.17	ND
RNF213	60	c.14576G>A (p.R4859K)	46/63 (47/126)	6/429 (6/858)	1.2×10^{-43}	298.1	190.8 (71.7–507.9)
FLJ35220		None					

Abbreviations: ND, not determined; SNP, single-nucleotide polymorphism.
[a]Nucleotide numbers of *RNF213* cDNA are counted from the A of the ATG initiator methionine codon (NCBI Reference sequence, NP_065965.4).
[b]*P*-values were calculated by Fisher's exact test.
[c]Genotypic distribution (carrier of the polymorphism vs non-carrier).

Table 3 Association of the p.R4859K (c.14576G>A) mutation with MMD

		Genotype		
	Total	*wt/wt (%)*	*wt/p.R4859K (%)*	*p.R4859K/ p.R4859K (%)[d]*
Members of 19 MMD families[a]				
Affected	42	0	39 (92.9)	3 (7.1)
Not affected	28	15 (53.6)	13 (46.4)	0
Individuals without a family history of MMD[b,c]				
Affected	63	17 (27.0)	45 (71.4)	1 (1.6)
Not affected	429	423 (98.6)	6 (1.4)	0

Abbreviations: MMD, moyamoya disease.
[a]Entire distribution, $\chi^2=29.4$, $P=4.2\times10^{-7}$.
[b]Entire distribution, $\chi^2=298.2$, $P=1.8\times10^{-65}$.
[c]Genotypic distribution (p.R4859K carrier vs non-carrier), $\chi^2=298.1$, $P=1.2\times10^{-43}$, odds ratio=190.8 (95% CI=71.7–507.9).
[d]The age of onset and initial symptoms of the four homozygotes were comparable to those of the 84 heterozygous patients.

in three patients heterozygous for the p.R4859K mutation (Figure 2b), excluding the possible instability of the mutant *RNF213* mRNA. Additional missense mutations, p.M3940V, p.V4616M and p.V4814M, were detected in three non-familial MMD cases without the p.R4859K mutation (Figure 2c). These mutations were not found in 388 control subjects and were detected in only one patient, suggesting that they were private mutations (Table 2). No copy number variation or mutation was identified in the *RNF213* locus of 12 MMD patients using comparative genome hybridization microarray analysis (Supplementary Figure 4). In total, 6 of the 429 control subjects (1.4%) were found to be heterozygous carriers of p.R4859K. Therefore, we concluded that the p.R4859K mutation increases the risk of MMD by a remarkably high amount (odds ratio=190.8 (95% confidence interval=71.7–507.9), $P=1.2\times10^{-43}$) (Table 3). It was recently reported that an SNP (ss161110142) in the promoter region of *RPTOR*, which is located ~150 kb downstream from *RNF213*, was associated with MMD.[17] Genotyping of the SNP in *RPTOR* showed that the *RNF213* p.R4859K mutation was more strongly associated with MMD than ss161110142 (Supplementary Figure 1).

RNF213 encodes a protein with 5256 amino acids harboring a RING (really interesting new gene) finger motif, suggesting that it functions as an E3 ubiquitin ligase (Figure 2c). It also has an AAA ATPase domain, which is characteristic of energy-dependent unfoldases.[18] To our knowledge, RNF213 is the first RING finger protein known to contain an AAA ATPase domain. The expression profile of *RNF213* has not been previously fully characterized. We performed a quantitative reverse transcription PCR analysis in various human tissues and cells. *RNF213* mRNA was highly expressed in immune tissues, such as spleen and leukocytes (Figure 3a and Supplementary Figure 5). Expression of *RNF213* was detected in fractions of both polymorphonuclear cells and mononuclear cells and was found in both B and T cell fractions (Supplementary Figure 6). A low but significant expression of *RNF213* was also observed in human umbilical vein endothelial cells and human pulmonary artery smooth muscle cells. Cellular expression was not enhanced in tumor cell lines, compared with leukocytes. In human fetal tissues, the highest expression was observed in leukocytes and the thymus (Supplementary Figure 6E). The expression of *RNF213* was surprisingly low in both adult and fetal brains. Overall, *RNF213* was ubiquitously expressed, and the highest expression was observed in immune tissues.

We studied the cellular expression of *Rnf213* in mice. The ISH analysis of spleen showed that *Rnf213* mRNA was present in small mononuclear cells, which were mainly localized in the white pulps (Figures 3b–g). The ISH signals were also detected in the primary follicles in the lymph node and in thymocytes in the medulla of the thymus (Supplementary Figure 7). To study *Rnf213* expression in activated lymphocytes we immunized mice with keyhole limpet hemocyanin, and examined *Rnf213* mRNA in spleen by ISH analysis. Primary immunization with keyhole limpet hemocyanin antigen revealed that the expression of *Rnf213* in the secondary follicle is as high as in the primary follicle in the lymph node (Supplementary Figure 8). In an E16.5 mouse embryo, expression was observed in the medulla of the thymus and in the cells around the mucous palatine glands (Supplementary Figure 9). These findings suggest that mature lymphocytes in a static state express *Rnf213* mRNA at a higher level than do their immature counterparts.

DISCUSSION

We identified a susceptibility locus for MMD by genome-wide and locus-specific association studies. Further sequencing analysis revealed a founder missense mutation in *RNF213*, p.R4859K, which was tightly associated with MMD onset. Identification of a founder mutation in individuals with MMD would resolve the following recurrent

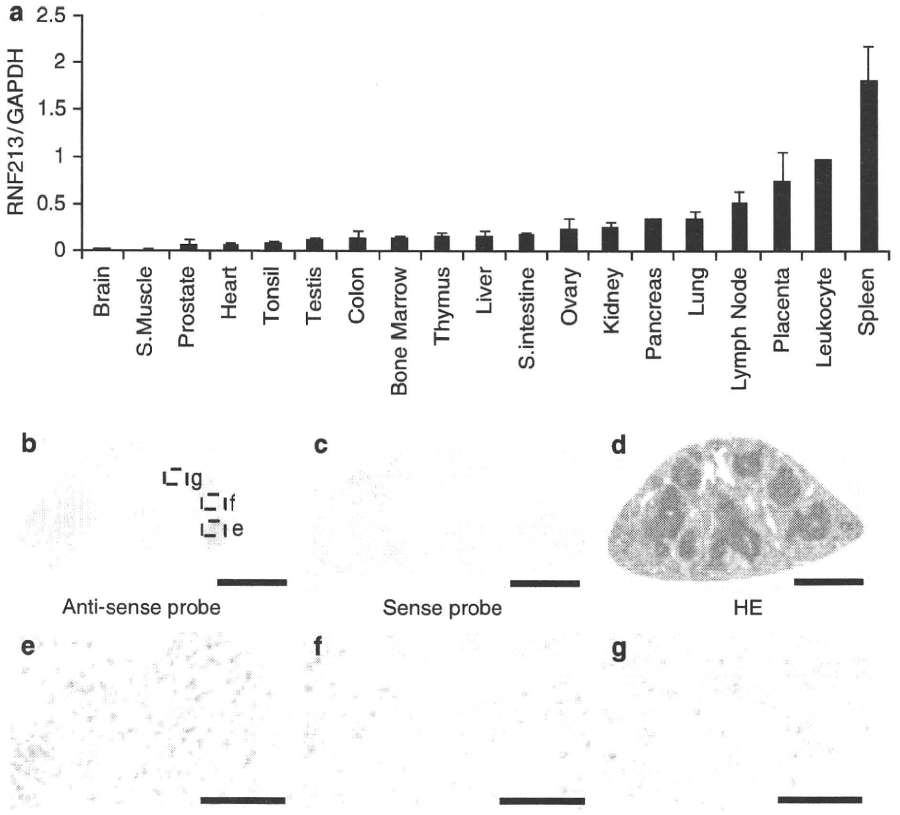

Figure 3 Expression of human RNF213 and murine Rnf213. (**a**) RT-PCR analysis of RNF213 mRNA in various human tissues. The expression levels of *RNF213* mRNA in various adult human tissues were evaluated by quantitative PCR using *GAPDH* mRNA as a control. The signal ratio of *RNF213* mRNA to *GAPDH* mRNA in each sample is shown on the vertical axis. (**b–g**) *In situ* hybridization (ISH) analysis of Rnf213 mRNA in mouse spleen. Specific signals for *Rnf213* mRNA were detected by ISH analysis with the anti-sense probe (**b**) but not with the sense probe (**c**). Hematoxylin–eosin staining of the mouse spleen (**d**). Signals for the *Rnf213* mRNA were observed in small mononuclear cells, which were mainly localized in the white pulps (dotted square, **e**) and partially distributed in the red pulps (dotted squares, **f** and **g**). Panels e, f and g show the high-magnification images of the corresponding fields in panel b. Scale bars, 1 mm (**b–d**) and 50 μm (**e–g**).

questions:[2,19] (i) why is MMD more prevalent in East Asia than in Western countries? The carrier frequency of p.R4859K in Japan is 1/72 (Table 2). In contrast, we found no p.R4859K carrier in 400 Caucasian controls (data not shown). Furthermore, no mutation was identified in five Caucasian patients with MMD after the full sequencing of *RNF213*. These results suggest that the genetic background of MMD in Asian populations is distinct from that in Western populations and that the low incidence of MMD in Western countries may be attributable to a lack of the founder *RNF213* mutation. (ii) Is unilateral involvement a subtype of MMD or a different disease?[2] We collected DNA samples from six patients with unilateral involvement and found a p.R4859K mutation in four of them (data not shown), suggesting that bilateral and unilateral MMD share a genetic background. (iii) Is pre-symptomatic diagnosis of MMD possible? In the present study, MMD never developed in the 15 mutation-negative family members in the 19 MMD families with the p.R4859K mutation (Table 3 and Supplementary Figure 1), suggesting the feasibility of presymptomatic diagnosis or exclusion by genetic testing.

How the mutant RNF213 protein causes MMD remains to be elucidated. The expression of *RNF213* was more abundant in a subset of leukocytes than in the brain, suggesting that blood cells have a function in the etiology of MMD. This observation agrees with a previous report that MMD patients have systemic angiopathy.[20] Recent studies have suggested that the postnatal vasculature can form through vasculogenesis, a process by which endothelial progenitor cell are recruited from the splenic pool and differentiate into mature endothelial cells.[21] Levels of endothelial progenitor cells in the peripheral blood are increased in MMD patients.[22] *RNF213* may be expressed in splenic endothelial progenitor cells and mutant *RNF213* might dysregulate the function of the endothelial progenitor cells. Further research is necessary to elucidate the role of *RNF213* in the etiology of MMD.

CONFLICT OF INTEREST

The authors declare no conflict of interest.

ACKNOWLEDGEMENTS

We thank all of the patients and their families for participating in this study. We also thank Dr Hidetoshi Ikeda at the Department of Neurosurgery, Tohoku University School of Medicine and Drs Toshiaki Hayashi and Reizo Shirane at the Department of Neurosurgery, Miyagi Children's Hospital, Sendai, Japan for patient recruitment. We are grateful to Ms Kumi Kato for technical assistance. This study was supported by grants from the Ministry of Education, Culture, Sports, Science and Technology, Japan and by the Research Committee on Moyamoya Disease of the Ministry of Health, Labor and Welfare, Japan.

1 Suzuki, J. & Takaku, A. Cerebrovascular 'moyamoya' disease. Disease showing abnormal net-like vessels in base of brain. *Arch. Neurol.* **20,** 288–299 (1969).
2 Suzuki, J. *Moyamoya Disease* (Springer-Verlag: Berlin, 1983).
3 Oki, K., Hoshino, H. & Suzuki, N. In: *Moyamoya Disease Update*, (eds Cho B.K., Tominaga T.) 29–34 (Springer: New York, 2010).
4 Phi, J. H., Kim, S. K., Wang, K. C. & Cho, B. K. In: *Moyamoya Disease Update*, (eds Cho B.K., Tominaga T). 82–86, (Springer: New York, 2010).
5 Yoshihara, T., Taguchi, A., Matsuyama, T., Shimizu, Y., Kikuchi-Taura, A., Soma, T. *et al.* Increase in circulating CD34-positive cells in patients with angiographic evidence of moyamoya-like vessels. *J. Cereb. Blood Flow Metab.* **28,** 1086–1089 (2008).
6 Achrol, A. S., Guzman, R., Lee, M. & Steinberg, G. K. Pathophysiology and genetic factors in moyamoya disease. *Neurosurg. Focus.* **26,** E4 (2009).
7 Scott, R. M. & Smith, E. R. Moyamoya disease and moyamoya syndrome.. *N. Engl. J. Med.* **360,** 1226–1237 (2009).
8 Kure, S. In: *Moyamoya Disease Update* (eds Cho B.K., Tominaga T.) 41–45 (Springer: Tokyo, 2010).
9 Kuriyama, S., Kusaka, Y., Fujimura, M., Wakai, K., Tamakoshi, A., Hashimoto, S. *et al.* Prevalence and clinicoepidemiological features of moyamoya disease in Japan: findings from a nationwide epidemiological survey. *Stroke.* **39,** 42–47 (2008).
10 Sakurai, K., Horiuchi, Y., Ikeda, H., Ikezaki, K., Yoshimoto, T., Fukui, M. *et al.* A novel susceptibility locus for moyamoya disease on chromosome 8q23. *J. Hum. Genet.* **49,** 278–281 (2004).
11 Nanba, R., Kuroda, S., Tada, M., Ishikawa, T., Houkin, K. & Iwasaki, Y. Clinical features of familial moyamoya disease. *Childs. Nerv. Syst.* **22,** 258–262 (2006).
12 Ikeda, H., Sasaki, T., Yoshimoto, T., Fukui, M. & Arinami, T. Mapping of a familial moyamoya disease gene to chromosome 3p24.2-p26. *Am. J. Hum. Genet.* **64,** 533–537 (1999).
13 Inoue, T. K., Ikezaki, K., Sasazuki, T., Matsushima, T. & Fukui, M. Linkage analysis of moyamoya disease on chromosome 6. *J. Child. Neurol.* **15,** 179–182 (2000).
14 Yamauchi, T., Tada, M., Houkin, K., Tanaka, T., Nakamura, Y., Kuroda, S. *et al.* Linkage of familial moyamoya disease (spontaneous occlusion of the circle of Willis) to chromosome 17q25.. *Stroke.* **31,** 930–935 (2000).
15 Wakai, K., Tamakoshi, A., Ikezaki, K., Fukui, M., Kawamura, T., Aoki, R. *et al.* Epidemiological features of moyamoya disease in Japan: findings from a nationwide survey. *Clin. Neurol. Neurosurg.* **99**(Suppl 2), S1–S5 (1997).
16 Mineharu, Y., Liu, W., Inoue, K., Matsuura, N., Inoue, S., Takenaka, K. *et al.* Autosomal dominant moyamoya disease maps to chromosome 17q25.3. *Neurology.* **70,** 2357–2363 (2008).
17 Liu, W., Hashikata, H., Inoue, K., Matsuura, N., Mineharu, Y., Kobayashi, H. *et al.* A rare Asian founder polymorphism of Raptor may explain the high prevalence of Moyamoya disease among East Asians and its low prevalence among Caucasians. *Environ. Health. Prev. Med.* **15,** 94–104 (2010).
18 Lupas, A. N. & Martin, J. AAA proteins.. *Curr. Opin. Struct. Biol.* **12,** 746–753 (2002).
19 Ikezaki, K. In: *Moyamoya disease* (eds Ikezaki K., Loftus C. M.) 43–75 (Thieme: New York, 2001).
20 Ikeda, E. Systemic vascular changes in spontaneous occlusion of the circle of Willis. *Stroke.* **22,** 1358–1362 (1991).
21 Zampetaki, A., Kirton, J. P. & Xu, Q. Vascular repair by endothelial progenitor cells. *Cardiovasc. Res.* **78,** 413–421 (2008).
22 Rafat, N., Beck, G., Pena-Tapia, P. G., Schmiedek, P. & Vajkoczy, P. Increased levels of circulating endothelial progenitor cells in patients with Moyamoya disease. *Stroke.* **40,** 432–438 (2009).

Supplementary Information accompanies the paper on Journal of Human Genetics website (http://www.nature.com/jhg)

Non-Hodgkin Lymphoma in a Patient With Cardiofaciocutaneous Syndrome

Akira Ohtake, MD, PhD, Yoko Aoki, MD, PhD,† Yuka Saito, MD,† Tetsuya Niihori, MD, PhD,† Atsushi Shibuya, MD, PhD,* Shigeo Kure, MD, PhD,† and Yoichi Matsubara, MD†*

Summary: Cardiofaciocutaneous (CFC) syndrome is a multiple congenital anomaly/mental retardation syndrome characterized by a distinctive facial appearance, ectodermal abnormalities, and heart defects. Clinically, it overlaps with both Noonan syndrome and Costello syndrome. Mutations in KRAS, BRAF, and MAP2K1/2 (MEK1/2) have been identified in patients with CFC syndrome. BRAF mutations are involved in more than 80% of CFC syndrome patients, and we have reported earlier that 2 CFC patients with BRAF mutations developed acute lymphoblastic leukemia. Here we report a boy with CFC syndrome who developed non-Hodgkin lymphoma. At 2 months of age, he developed pneumonia with pleurisy and was diagnosed as having non-Hodgkin lymphoma (precursor T-cell lymphoblastic lymphoma) by cytopathologic examination of the pleural fluid. He was suspected of having Noonan syndrome because of his facial appearance, webbed neck, and cubitus valgus. Precursor T-cell lymphoblastic lymphoma was treated by the TCCSG NHL 94-04 protocol. At 9 years of age, he was clinically reevaluated and diagnosed as having CFC syndrome because of his distinctive facial appearance, multiple nevi, and moderate mental retardation. Sequencing analysis showed a germline p.A246P (c.736G > C) mutation in BRAF reported earlier in CFC syndrome. Molecular diagnosis and careful observation should be considered in children with CFC syndrome.

Key Words: RAF, RAS-MAPK, non-Hodgkin lymphoma, cardiofaciocutaneous syndrome, Noonan syndrome, KRAS, BRAF, leukemia

(*J Pediatr Hematol Oncol* 2010;00:000–000)

Cardiofaciocutaneous (CFC) syndrome is a multiple congenital anomaly/mental retardation syndrome characterized by heart defects, facial dysmorphism, ectodermal abnormalities, and mental retardation.[1,2] Typical facial characteristics include a high forehead with bitemporal constriction, hypoplastic supraorbital ridges, downslanting palpebral fissures, a depressed nasal bridge, and posteriorly angulated ears with prominent helices. Affected individuals present with heart defects, including pulmonic stenosis, atrial septal defects, and hypertrophic cardiomyopathy. Ectodermal abnormalities including sparse, friable hair, multiple nevi, and hyperkeratotic skin lesions are noted. CFC syndrome has many clinical features in common with those of Noonan syndrome and Costello syndrome. Of these 3 syndromes, Noonan syndrome is most frequent, its incidence is estimated to be 1 in 1000 to 1 in 2500 live births. Compared with the other 2 syndromes, Noonan syndrome has lower frequencies of mental retardation (24% to 35%), heart defects (50% to 67%), and skin abnormalities (2% to 27%),[3] whereas CFC patients show a high frequency of growth failure (78.9%), mental retardation (100%), heart defects (84.2%), and skin abnormalities (68.4%).[2] Costello syndrome is characterized by mental retardation, high birth weight, neonatal feeding problems, curly hair, redundant skin, nasal papillomata, and tumor predisposition. Wrinkled palms and soles, hyperpigmentation, and joint hyperextension, which have been commonly reported in Costello syndrome but not in CFC syndrome, have been observed in 30% to 40% of the mutation-positive CFC patients.[4] Thus, differential diagnosis of these syndromes is difficult because of their overlapping clinical manifestations.

Mutations in molecules in the RAS/mitogen-activated protein kinase (MAPK) pathway have been identified in these disorders: HRAS in Costello syndrome[5]; *PTPN11*, *KRAS*, *SOS1*, *RAF1*, and *NRAS* in Noonan syndrome[6–12]; and *KRAS*, *BRAF*, and *MAP2K1/2* in individuals with CFC syndrome.[2,13] Therefore, these syndromes are termed NCFC syndrome or RAS/MAPK syndromes.[14,15] Approximately 10% of patients with Costello syndrome have been shown to have malignant tumors, including neuroblastoma, rhabdomyosarcoma, and bladder carcinoma. For Costello syndrome, tumor-screening protocols have been proposed.[16] In contrast, little attention has been paid to the development of tumors in patients with CFC syndrome.

Herein we report a Japanese patient with CFC syndrome who developed non-Hodgkin lymphoma (NHL) at 2 months of age. Although he had been suspected of having Noonan syndrome, reevaluation of the clinical manifestations and identification of a BRAF mutation led to a re-diagnosis of CFC syndrome. Our observations, together with a literature review of earlier patients, suggest the importance of the careful observation for malignancy in CFC syndrome.

CASE REPORT

The propositus was a 12-year-old Japanese boy. He was the first son of unrelated healthy parents. At birth, his father was 27 years old, as was his mother. The baby was delivered at 40 weeks by obstetrical vacuum extraction and its birth weight was 3488 g (+0.8 SD), length was 49.6 cm (+0.1 SD), and occipitofrontal circumference was 35 cm (+1.0 SD). At 2 months of age, coughing, rhinorrhea, and feeding difficulty were observed. He was admitted

Received for publication October 29, 2009; accepted February 19, 2010.
From the *Department of Pediatrics, Saitama Medical University, Moroyama, Saitama; and †Department of Medical Genetics, Tohoku University School of Medicine, Sendai, Japan.
This work was supported by grants-in-aid from Japan Society for the Promotion of Science and from the Ministry of Health, Labor, and Welfare of Japan. The authors have no financial interest in the outcome of this study.
Reprints: Yoko Aoki, MD, PhD, Department of Medical Genetics, Tohoku University School of Medicine, 1-1 Seiryo-machi, Sendai 980-8574, Japan (e-mail: aokiy@mail.tains.tohoku.ac.jp).

to our hospital because his chest roentgenogram showed right lung pneumonia with pleurisy. Echocardiography was normal and a computed tomography scan showed right atelectasis and right pleural effusion. There were no mediastinal or axillary lymphadenopathies. Laboratory findings were as follows: hemoglobin 10.4 g/dL, white blood cells 9.1×10^9/L, and platelets 404×10^9/L. The levels of serum lactate dehydrogenase and C-reactive protein were normal. Pleural effusion aspirate had a milky-white appearance, a triglyceride content of 2529 mg/dL, and a lactate dehydrogenase level of 1656 IU/dL. Cytologic examination of the pleural fluid showed highly cellular specimens. The majority of these cells were lymphoblasts. These cells showed T-cell phenotype: positive for CD2, CD3, CD5, and CD7 by an immunophenotyping study using flow cytometry. No other infiltration was identified by computed tomography /magnetic resonance imaging, bone marrow aspiration, and Garium scintigram. He was then diagnosed as having T-cell lymphoblastic lymphoma by cytopathologic examination of the pleural fluid (stage III). At admission, the patient was diagnosed as having Noonan syndrome because of the following anomalies: hypertelorism, downslanting palpebral fissures, low nasal bridge, low set and posterior rotated ears, micrognathia, short and webbed neck, cubitus vulgus, funnel chest, and wide nipples. His chromosomal analyses of both peripheral lymphocytes and lymphoma cells showed a normal karyotype of 46, XY.

Induction therapy, which consisted of vincristine, predonisolone, tetrahydropyranyl adriamycin, cyclophosphamide, and *Escherichia coli* asparaginase, was performed for 3 months. The patient had a good clinical response to the chemotherapy, which was terminated before the entire protocol was finished. No relapse was observed afterwards.

At the age of 9 years, he had a distinctive facial appearance, including hypertelorism, underdeveloped supraorbital ridges, sparse and highly arched eyebrows, bilateral ptosis, depressed nasal bridge, concave nasal ridge, broad nasal base, anteverted nares, long philtrum, everted lower lip, and low set and posterior rotated ears (Fig. 1). Other features included a webbed/short neck, multiple nevi in his face, cubitus valgus, pectus excavatum, widely spaced nipples, and short stature of −3.1 SD. Results of growth hormone provocation tests with arginine and insulin were both normal. Echocardiography and ECG revealed no cardiac abnormalities. His intelligent quotient has not been accurately examined, but he attends a class for the handicapped. At 9 years of age, he was suspected of having CFC syndrome because of his facial appearance, mental retardation, and multiple nevi, although no heart defects were noted.

FIGURE 1. Facial appearance of the patient.

Mutation Analysis

Genomic DNA from blood leukocytes from the patient was isolated by a standard protocol. Fifteen exons with flanked introns in which the mutations have been identified in CFC patients and *HRAS* exon1, in which mutations are clustered in more than 90% of patients with Costello syndrome, were examined and amplified by polymerase chain reaction. These were exons 1, 2, and 5 in *KRAS*; exons 6 and 11 to 16 in *BRAF*; exons 2 and 3 in *MAP2K1*; and exons 2, 3, and 7 in *MAP2K2*.[2,4] The polymerase chain reaction products were gel purified and sequenced on an ABI PRISM 310 automated DNA sequencer (Applied Biosystems). This study was approved by the Ethics Committee of the Tohoku University School of Medicine. We obtained informed consent for the sample and specific consent for a photograph. Sequencing analysis showed a G-to-C change at nucleotide 736, resulting in an A246P mutation of BRAF in the heterozygous form.

DISCUSSION

The patient with CFC syndrome herein reported developed right lung pneumonia with pleurisy at 2 months of age. He was first diagnosed as having Noonan syndrome. The cytopathologic examination of lymphoblasts in the pleural fluid showed T-cell phenotype and the patient was diagnosed as having precursor T-cell lymphoblastic lymphoma. At 9 years of age, a *BRAF* A246P mutation was identified in the patient. We concluded that the patient had CFC syndrome because of his distinctive facial features, including underdeveloped supraorbital ridges, sparse and highly arched eyebrows, ptosis, growth failure, moderate mental retardation, and multiple nevi in skin, although no heart defects were observed.

Mutations in *BRAF* identified in CFC patients partially overlap those identified in cancers. V600E mutation, which is most frequently identified in cancers, has never been detected in CFC patients and activation of downstream extracellular signal-regulated kinase is weaker in germline mutations than in V600E.[15] The association with malignancy is rarer in CFC syndrome than in Costello syndrome with germline *HRAS* mutations, 10% of which develop malignant tumors including rhabdomyosarcoma, neuroblastoma, and bladder carcinoma. Four patients with CFC syndrome have been found to develop malignant tumors (Table 1). We have earlier reported 2 patients with *BRAF* mutations who developed acute lymphoblastic leukemia (ALL).[2,18] A CFC patient with a MEK1 mutation has been reported to have developed hepatoblastoma after cardiac transplantation.[19] To date, 104 CFC patients with *BRAF* mutations and 42 with CFC patients with MEK1/2 mutations have been reported.[15] The frequency of the association with malignant tumors cannot be neglected. Careful observation should be considered in children with CFC syndrome and related disorders.

Precursor T-cell lymphoblastic lymphoma accounts for approximately 33% of pediatric NHL and most commonly involves the mediastinum and lymph nodes.[20] The precise incidence of NHL in children is not known and the development of NHL in the early infantile period is rare.[21] It is possible that our patient developed NHL at 2 months of age owing to having the germline mutation in the proto-oncogene *BRAF*.

The contribution of somatic mutations in BRAF to hematologic malignancy has been controversial. Lee et al[22] identified BRAF mutations in 4 cases with diffuse large

TABLE 1. Summary of CFC Patients who Developed Malignant Tumors

	1[2,17]	2[18]	3 (Current Study)	4[19]
Gene	*BRAF*	*BRAF*	*BRAF*	MEK1
Amino acid change	G469E	E501G	A246P	Y130C
Clinical manifestations				
Clinical diagnosis	CFC	CFC	Noonan (2 months of age), CFC (9 y)	Costello (6 wk) CFC
Heart defects	Mild PS, ASD, and asymmetrical hypertrophy of the interventricular septum	Patent ductus arteriosus and asymmetrical hypertrophy of the interventricular septum	No	Heart transplantation owing to severe hypertrophic cardiomyopathy (8 mo of age), a small anterior muscular septal defect
Skin and hair	Keratosis pilaris (3 y) cafe au lait spots, sparse, friable hair	Generalized pigmentation and patchy hyperkeratosis, sparse curly hair	Multiple nevi (9 y)	Loose plantar and palmer skin with deep creases, sparse thin hair
Mental and growth development	Moderate mental retardation	Severe mental retardation	Moderate mental retardation, short stature (−3.1 SD)	Developmental delay
Other		Bilateral cryptorchidism		
Hematologic malignancy	ALL	ALL	Precursor T-lymphoblastic lymphoma	Hepatoblastoma
Age at diagnosis	5 y	1 y 9 mo	2 mo	35 mo
Initial symptoms	hepatosplenomegaly	hepatosplenomegaly and right testicular swelling	Coughing, rhinorrhea, and feeding difficulty	Progressive dyspnea, systolic murmur, and hepatomegaly
Laboratory findings/ imagings	8% of 1.4×10^9/L leukocytes in peripheral blood, 98% lymphoblasts in bone marrow: positive for TdT, HLA-DR, CD34, CD13, CD33, CD19, CD10, CD22, and CD79	100% of 8.3×10^{10}/L leukocytes in peripheral blood, 98% lymphoblasts in bone marrow: positive for TdT, HLA-DR, CD19, CD10, CD22, and CD79	Right lung pneumonia with pleurisy; cytologic examination of pleural fluid showed T-cell lymphoblasts: positive for CD2, CD3, CD5, and CD7	Intracardiac mass in the right atrium, extending into the inferior vena cava, to a level close to the renal veins; 5.2×6.4 cm intrahepatic mass infiltrating the posterior branch of the right portal vein and extending into the right hepatic lobe
Treatment	Vincristine, dexamethasone and *E. coli* asparginase for induction therapy	Vincristine, predonsolone, *E. coli* asparginase, and doxorubicin for induction therapy	Vincristine, predonisolone, tetrahydropyranyl adriamycin, cyclophosphamide, and *E. coli* asparaginase	Surgical dissection of intracardiac mass revealed hepatoblastoma, cisplatin, vincristine, and 5-flurouracil as chemotherapy
Outcome	Healthy at 15 y of age	Healthy as of age 9 y 3 mo	Healthy as of age 12 y 4 mo	Died at 35 mo

ALL indicates acute lymphoblastic leukemia; ASD, atrial septal defect; CFC, cardiofaciocutaneous syndrome; E. coli, Escherichia coli; HLA_DR, human leucocyte antigen-DR; PS, pulmonic stenosis; TdT, terminal deoxynucleotidyl transferase.

TABLE 2. *BRAF* Mutations Identified in Hematologic Malignancies

Nucleotide Change	Amino Acid Change	Malignant Tumor	References
c. 1402 G > C	p.G468R	Diffuse large B-cell lymphoma	22
c. 1403 G > C	p.G468A	Diffuse large B-cell lymphoma	22
c. 1403 G > C	p.G468A	Diffuse large B-cell lymphoma	22
c. 1403 G > C	p.G468A	B-cell ALL	23
c. 1403 G > C	p.G468A	B-cell ALL	23
c. 1403 G > C	p.G468A	Bisphenotypic acute leukemia	23
c. 1403 G > C	p.G468A	AML	23
c. 1768G > A	p.V590I	Pre-B ALL	24
c. 1778A > G	p.D593G	Diffuse large B-cell lymphoma	22
c. 1786G > A	p.G596S	T-ALL	24
c. 1790T > A	p.L597Q	Pre-B ALL	24
c. 1790T > A	p.L597Q	Pre-B ALL	24
c. 1790T > A	p.L597Q	Pre-B ALL	24
—	p.V600E	U266 myeloma cells	25, 26
c.1796T > A	p.V600E	t-AML(M5)	27
c.1796T > A	p.V600E	t-AML(M5)	27
c.1796T > A	p.V600E	t-AML(M5)	27
c.1796T > A	p.V600E	T-ALL	24

ALL indicates acute lymphoblastic leukemia; t-AML, therapy-related acute myeloid leukemia; T-ALL, T-cell ALL.

B-cell lymphoma (2 cases with G468A, 1 with G468R, and 1 with D593G) and 4 cases with leukemia (G468A) (Table 2).[23] Gustafsson et al[24] investigated exons 11 and 15 of *BRAF* in 29 cases with pre-B ALL (25 cases), T-cell ALL (3 cases), and undifferentiated ALL (1 case) and identified *BRAF* mutations in 6 cases (21%). Christiansen et al[27] identified 3 BRAF mutations in 3 of 51 therapy-related acute myeloid leukemia patients, but not in therapy-related myelodysplasia. In contrast, Davidsson et al[28] did not identify any BRAF mutations in 92 B-cell precursor ALL and 17 T-cell ALL. In other studies, no *BRAF* mutations were identified in 86 cases with childhood ALL,[29] in 104 cases with acute myeloid leukemia, [30] and in 65 cases with juvenile myelomonocytic leukemia.[31] Recently, it has been postulated that 2 general types of gene mutation cooperate to produce leukemogenesis.[32] Class I mutations are those with receptor tyrosine kinases or genes downstream in the RAS/RAF/MEK/extracellular signal-regulated kinase pathway, which result in a proliferative or survival advantage. Class II mutations impair hematologic differentiation. BRAF is a member of the RAF serine/threonine family and transmits the RAS signal to downstream MEK/ERK. Somatic mutations in *BRAF* have been identified in approximately 7% of tumors, including malignant melanoma, pancreatic tumors, and lung cancer.[2] BRAF mutations are involved in Class I mutation and possibly contribute to leukemogenesis.

ACKNOWLEDGMENTS

The authors thank the patient and his family who participated in this study. The patient's parents have given permission for the use of the figure in the article. They also thank Dr Raoul CM Hennekam for informing us about the outcome of his patient.

REFERENCES

1. Reynolds JF, Neri G, Herrmann JP, et al. New multiple congenital anomalies/mental retardation syndrome with cardio-facio-cutaneous involvement–the CFC syndrome. *Am J Med Genet.* 1986;25:413–427.
2. Niihori T, Aoki Y, Narumi Y, et al. Germline KRAS and BRAF mutations in cardio-facio-cutaneous syndrome. *Nat Genet.* 2006;38:294–296.
3. Wieczorek D, Majewski F, Gillessen-Kaesbach G. Cardio-facio-cutaneous (CFC) syndrome—a distinct entity? Report of three patients demonstrating the diagnostic difficultics in delineation of CFC syndrome. *Clin Genet.* 1997;52:37–46.
4. Narumi Y, Aoki Y, Niihori T, et al. Molecular and clinical characterization of cardio-facio-cutaneous (CFC) syndrome: overlapping clinical manifestations with Costello syndrome. *Am J Med Genet A.* 2007;143A:799–807.
5. Aoki Y, Niihori T, Kawame H, et al. Germline mutations in HRAS proto-oncogene cause Costello syndrome. *Nat Genet.* 2005;37:1038–1040.
6. Tartaglia M, Pennacchio LA, Zhao C, et al. Gain-of-function SOS1 mutations cause a distinctive form of Noonan syndrome. *Nat Genet.* 2007;39:75–79.
7. Tartaglia M, Mehler EL, Goldberg R, et al. Mutations in PTPN11, encoding the protein tyrosine phosphatase SHP-2, cause Noonan syndrome. *Nat Genet.* 2001;29:465–468.
8. Roberts AE, Araki T, Swanson KD, et al. Germline gain-of-function mutations in SOS1 cause Noonan syndrome. *Nat Genet.* 2007;39:70–74.
9. Razzaque MA, Nishizawa T, Komoike Y, et al. Germline gain-of-function mutations in RAF1 cause Noonan syndrome. *Nat Genet.* 2007;39:1013–1017.
10. Pandit B, Sarkozy A, Pennacchio LA, et al. Gain-of-function RAF1 mutations cause Noonan and LEOPARD syndromes with hypertrophic cardiomyopathy. *Nat Genet.* 2007;39:1007–1012.
11. Schubbert S, Zenker M, Rowe SL, et al. Germline KRAS mutations cause Noonan syndrome. *Nat Genet.* 2006;38:331–336.
12. Cirstea IC, Kutsche K, Dvorsky R, et al. A restricted spectrum of NRAS mutations causes Noonan syndrome. *Nat Genet.* 2010;42:27–29.
13. Rodriguez-Viciana P, Tetsu O, Tidyman WE, et al. Germline mutations in genes within the MAPK pathway cause cardio-facio-cutaneous syndrome. *Science.* 2006;311:1287–1290.
14. Bentires-Alj M, Kontaridis MI, Neel BG. Stops along the RAS pathway in human genetic disease. *Nat Med.* 2006;12:283–285.
15. Aoki Y, Niihori T, Narumi Y, et al. The RAS/MAPK syndromes: novel roles of the RAS pathway in human genetic disorders. *Hum Mutat.* 2008;29:992–1006.
16. Gripp KW, Scott CI Jr, Nicholson L, et al. Five additional Costello syndrome patients with rhabdomyosarcoma: proposal for a tumor screening protocol. *Am J Med Genet.* 2002;108:80–87.
17. van Den Berg H, Hennekam RC. Acute lymphoblastic leukaemia in a patient with cardiofaciocutaneous syndrome. *J Med Genet.* 1999;36:799–800.
18. Makita Y, Narumi Y, Yoshida M, et al. Leukemia in Cardio-facio-cutaneous (CFC) syndrome: a patient with a germline mutation in BRAF proto-oncogene. *J Pediatr Hematol Oncol.* 2007;29:287–290.
19. Al-Rahawan MM, Chute DJ, Sol-Church K, et al. Hepatoblastoma and heart transplantation in a patient with cardio-facio-cutaneous syndrome. *Am J Med Genet A.* 2007;143A:1481–1488.
20. Smock KJ, Nelson M, Tripp SR, et al. Characterization of childhood precursor T-lymphoblastic lymphoma by immunophenotyping and fluorescent in situ hybridization: a report from the Children's Oncology Group. *Pediatr Blood Cancer.* 2008;51:489–494.
21. Mann G, Attarbaschi A, Burkhardt B, et al. Clinical characteristics and treatment outcome of infants with non-Hodgkin lymphoma. *Br J Haematol.* 2007;139:443–449.

22. Lee JW, Yoo NJ, Soung YH, et al. BRAF mutations in non-Hodgkin's lymphoma. *Br J Cancer.* 2003;89:1958–1960.
23. Lee JW, Soung YH, Park WS, et al. BRAF mutations in acute leukemias. *Leukemia.* 2004;18:170–172.
24. Gustafsson B, Angelini S, Sander B, et al. Mutations in the BRAF and N-ras genes in childhood acute lymphoblastic leukaemia. *Leukemia.* 2005;19:310–312.
25. Velangi M, Matheson E, Taylor P, et al. BRAF gene is not mutated in mismatch repair-proficient or -deficient plasma cell dyscrasias. *Leukemia.* 2004;18:658–659.
26. Ng MH, Lau KM, Wong WS, et al. Alterations of RAS signalling in Chinese multiple myeloma patients: absent BRAF and rare RAS mutations, but frequent inactivation of RAS SF1A by transcriptional silencing or expression of a non-functional variant transcript. *Br J Haematol.* 2003;123:637–645.
27. Christiansen DH, Andersen MK, Desta F, et al. Mutations of genes in the receptor tyrosine kinase (RTK)/RAS-BRAF signal transduction pathway in therapy-related myelodysplasia and acute myeloid leukemia. *Leukemia.* 2005;19:2232–2240.
28. Davidsson J, Lilljebjorn H, Panagopoulos I, et al. BRAF mutations are very rare in B- and T-cell pediatric acute lymphoblastic leukemias. *Leukemia.* 2008;22:1619–1621.
29. Case M, Matheson E, Minto L, et al. Mutation of genes affecting the RAS pathway is common in childhood acute lymphoblastic leukemia. *Cancer Res.* 2008;68:6803–6809.
30. Smith ML, Snaddon J, Neat M, et al. Mutation of BRAF is uncommon in AML FAB type M1 and M2. *Leukemia.* 2003; 17:274–275.
31. de Vries AC, Stam RW, Kratz CP, et al. Mutation analysis of the BRAF oncogene in juvenile myelomonocytic leukemia. *Haematologica.* 2007;92:1574–1575.
32. Komeno Y, Kitaura J, Kitamura T. Molecular bases of myelodysplastic syndromes: lessons from animal models. *J Cell Physiol.* 2009;219:529–534.

Journal of the Neurological Sciences xxx (2010) xxx–xxx

Contents lists available at ScienceDirect

Journal of the Neurological Sciences

journal homepage: www.elsevier.com/locate/jns

Short communication

Cervical pachymeningeal hypertrophy as the initial and cardinal manifestation of mucopolysaccharidosis type I in monozygotic twins with a novel mutation in the alpha-l-iduronidase gene

Yutaka Furukawa [a,*], Ayumi Hamaguchi [a], Ichiro Nozaki [a], Takashi Iizuka [a], Takeshi Sasagawa [b], Yosuke Shima [b], Satoru Demura [b], Hideki Murakami [b], Norio Kawahara [b], Torayuki Okuyama [c], Kazuo Iwasa [a], Masahito Yamada [a]

[a] Department of Neurology and Neurobiology of Aging, Kanazawa University Graduate School of Medical Science, Kanazawa, Japan
[b] Department of Orthopaedic Surgery, Kanazawa University Hospital, Kanazawa, Japan
[c] Department of Clinical Laboratory Medicine, National Center for Child Health and Development, Tokyo, Japan

ARTICLE INFO

Article history:
Received 24 June 2010
Received in revised form 20 November 2010
Accepted 23 November 2010
Available online xxxx

Keywords:
Mucopolysaccharidosis type I
Pachymeningeal hypertrophy
Cervical myelopathy
Monozygotic twin
Alpha-L-iduronidase gene mutation

ABSTRACT

We describe a pair of monozygotic twins with an attenuated form of mucopolysaccharidosis type I (MPS-I). At age 24, they both developed cervical myelopathy as a cardinal manifestation. They each also had mild valve abnormalities and both inguinal and umbilical hernia, however, other characteristic features of MPS-I were absent or very mild. Magnetic resonance imaging revealed the cervical cord compressed by pachymeningeal hypertrophy. Surgery with dural plasty and laminoplasty resulted in decompression of the cervical cord with clinical improvement, revealing marked thickening of the dura mater. Both patients showed a marked decrease of alpha-L-iduronidase (IDUA) activity with c.252insC (p.P55fsX62; known) and c.1209C>A (p.T374N; novel) mutations of the IDUA gene (*IDUA*). Patients with MPS-I have been reported to present with various clinical phenotypes and severities even if they have identical mutations of *IDUA*. The quite similar, unique phenotype in monozygotic twins suggests that not only *IDUA* mutation but also other genetic factors than *IDUA* markedly influence the clinical manifestations of MPS-I.

1. Introduction

Mucopolysaccharidosis type I (MPS-I) is an autosomal recessive disorder caused by a deficiency of α-L-iduronidase (IDUA), which leads to the accumulation of dermatan sulfate and heparan sulfate throughout the body. The IDUA gene (*IDUA*) is located on chromosome 4p 16.3 containing 14 exons [1], and approximately 100 mutations of *IDUA* have been identified [2]. MPS-I presents with various clinical manifestations including valve abnormality, joint contracture, corneal clouding, and course facial features [3]. Some patients with MPS-I have been reported to show cervical myelopathy due to cervical pachymeningeal hypertrophy during their clinical course [4,5]; however, cervical myelopathy is rare as the initial and cardinal manifestation of MPS-I.

We describe monozygotic twins with an attenuated form of MPS-I associated with a novel mutation of *IDUA*, who both showed cervical myelopathy as the initial and cardinal manifestation.

2. Case report

2.1. Patient 1

A 24-year-old Japanese man was admitted because of a 6-month history of progressive gait disturbance. He was born from non-consanguineous, young and healthy parents. He had a healthy elder brother and an affected twin brother (Patient 2). Pregnancy and labor had been uneventful, and birth weight was 2300 g. Mental and motor development were normal, and he had graduated from a vocational school. Past medical histories included Kawasaki disease at age 6 months, and inguinal hernia treated by surgical repair in childhood and again at age 20.

Physical examination demonstrated a height of 156.6 cm (mean height of Japanese male at age 24 is 170.9 ± 6.0 (SD) cm according to the National Health and Nutrition Survey in Japan, 2006), body weight of 45.8 kg (mean body weight of Japanese male at age 24 is 62.6 ± 9.8 (SD) kg according to the National Health and Nutrition Survey in Japan, 2006), systolic ejection heart murmur and umbilical hernia. Joint contractures, enlargements of tonsils and tongue, hepatomegaly and splenomegaly were all absent. Corneal clouding evaluated by ophthalmologist with slip lamp was also absent, and the facial features were normal. On neurologic examination, both

* Corresponding author. Department of Neurology and Neurobiology of Aging, Kanazawa University Graduate School of Medical Science, 13-1, Takara-machi, Kanazawa, Ishikawa 920-8640, Japan. Tel.: +81 76 265 2292; fax: +81 76 234 4253.
E-mail address: furukawa@med.kanazawa-u.ac.jp (Y. Furukawa).

0022-510X/$ – see front matter © 2010 Elsevier B.V. All rights reserved.
doi:10.1016/j.jns.2010.11.022

Please cite this article as: Furukawa Y, et al, Cervical pachymeningeal hypertrophy as the initial and cardinal manifestation of mucopolysaccharidosis type I in monozygotic twins with a novel mutation..., J Neurol Sci (2010), doi:10.1016/j.jns.2010.11.022

legs were markedly spastic with a scissors gait. Deep tendon reflexes were mildly exaggerated in the upper extremities, and markedly exaggerated in the lower extremities with bilateral Babinski signs.

Findings on urinalysis, routine hematological and blood chemistry examinations were all normal. Urine chemistry examination demonstrated increased excretion of uronic acid (63.1 mg/g creatinine; normal range 8.3–12.3 mg/g creatinine). Electrocardiogram was normal, and nerve conduction studies (NCS) on bilateral median nerve showed no evidence of carpal tunnel syndrome. Radiography of the chest demonstrated mild thoracic deformity (Fig. 1A) and that of cervical spine demonstrated hypoplasia of vertebral body and spinous process (Fig. 1B). Transthoracic echocardiogram (TTE) demonstrated mild aortic valve stenosis (1.2 cm^2 of average valve area (AVA)) with pressure gradient (PG) across the aortic valve of 33.6 mm Hg with normal wall motion of the left ventricle. Magnetic resonance image (MRI) of the cervical spine showed severe cervical cord compression due to thickening of the surrounding dura mater without gadolinium enhancement at C2-6 levels (Fig. 2A, C, E). Brain MRI demonstrated enlarged perivascular space and small hyperintense lesions on fluid attenuated inversion recovery image (Fig. 3A, C, E). There is no dural thickening in intracranial, thoracic, and lumbar region. Cerebrospinal fluid (CSF) examinations demonstrated an elevated protein level (440 mg/dL; normal range 10–40 mg/dL), which would be resulted from CSF circulatory disturbance caused by severe spinal canal stenosis, without pleocytosis. Cytology and culture for bacteria and mycobacteria were negative. Wechsler Adult Intelligence Scale Third Edition (WAIS-III) demonstrated overall intelligence quotient (IQ) of 101, verbal IQ of 93 and performance IQ of 112.

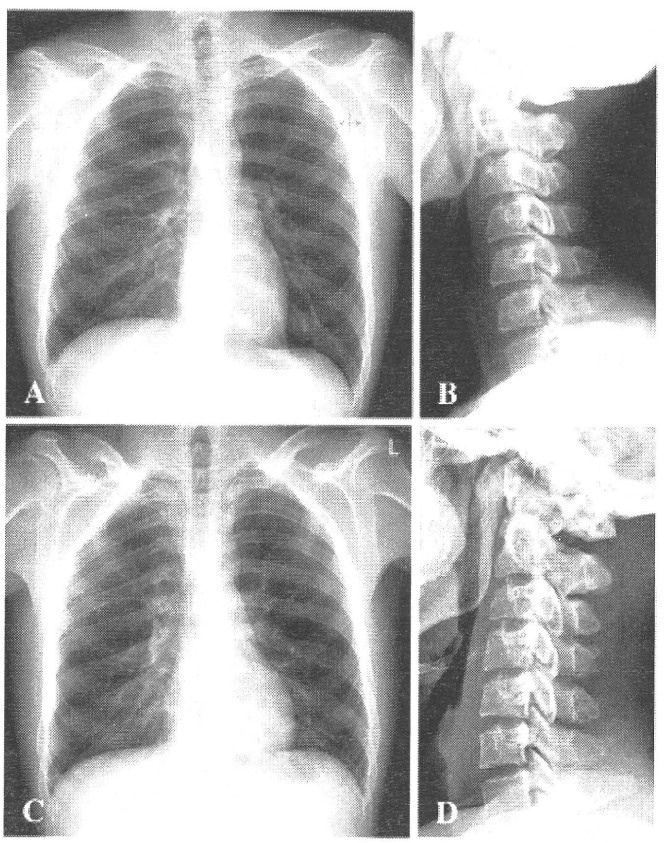

Fig. 1. Radiographies of the chest and cervical spine of Patients 1 (A, B) and 2 (C, D) showed mild thoracic deformity (A, C), and mild hypoplasia of vertebral body and spinous process (B, D).

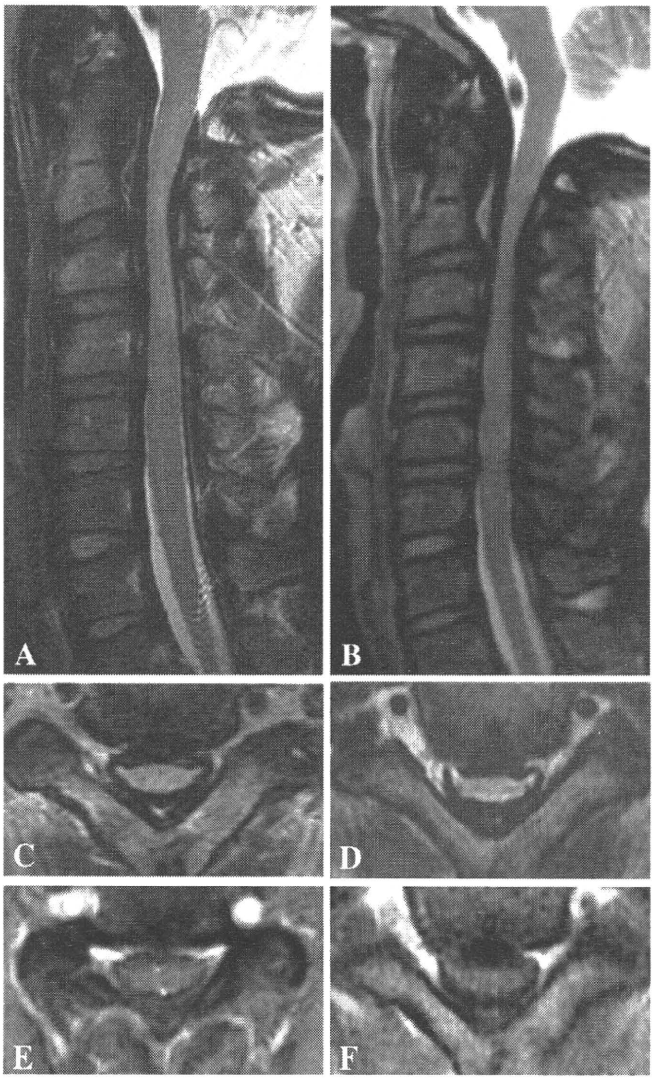

Fig. 2. MRI of the cervical spine of Patients 1 (A, C, E) and 2 (B, D, F) showed severe cord compression at C2-6, surrounded by thickened dura mater. The thickened dura was characterized by hypointensities on both T1- and T2-weighted images, but there was no gadolinium enhancement (A–D: T2-weighted image; E, F: T1-weighted image with gadolinium enhancement; C–F: axial sections at C2/3 level).

2.2. Patient 2

A 24-year-old man, the twin brother of Patient 1, was admitted to our ward because of a 3-month history of progressive gait disturbance. Onset was 6 months after the development of gait disturbance in Patient 1. Birth weight was 1900 g and mental and motor development were both normal. He had graduated from high school. Past medical histories included inguinal hernia treated by surgical repair at 2 months of age and bronchial asthma since 4 years of age.

Physical examination demonstrated a height of 157.0 cm, body weight of 45.3 kg, systolic ejection heart murmur, umbilical hernia, and minor joint contractures of the elbow and knee. Enlargements of tonsils and tongue, hepatomegaly and splenomegaly were all absent. Corneal clouding evaluated by ophthalmologist with slip lamp was also absent, and the facial features were normal. On neurologic examination, both legs were markedly spastic with spastic gait. He had mild hypoesthesia below the sensory level around C5. Romberg sign was positive. Exaggeration of deep tendon reflexes was slight in the upper extremities, and marked in the lower extremities with bilateral Babinski signs.

Please cite this article as: Furukawa Y, et al, Cervical pachymeningeal hypertrophy as the initial and cardinal manifestation of mucopolysaccharidosis type I in monozygotic twins with a novel mutation..., J Neurol Sci (2010), doi:10.1016/j.jns.2010.11.022

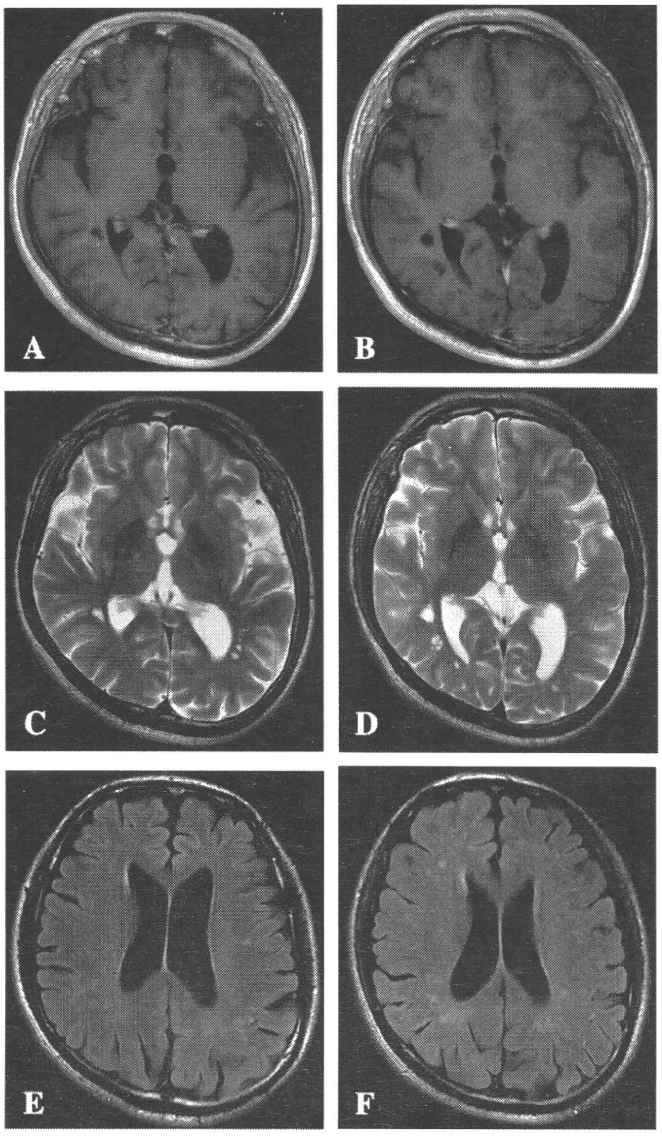

Fig. 3. Brain MRI of Patients 1 (A, C, E) and 2 (B, D, F) showed enlarged perivascular space around the posterior horn of the lateral ventricle (A–D), and small hyperintense lesions in deep white matter (E, F). There is no thickening and abnormal enhancement of the intracranial dura mater (A, B: T1-weighted image with gadolinium enhancement; C, D: T2-weighted image; E, F: fluid attenuated inversion recovery image).

Urinalysis, routine hematological and blood chemistry examinations all showed normal findings. Urine chemistry examination demonstrated increased excretion of uronic acid (51.7 mg/g creatinine). Radiographies of chest and cervical spine showed similar findings to those in Patient 1 (Fig. 1C, D). Electrocardiogram showed increased amplitude of QRS complex without ST changes. NCS on bilateral median nerve did not show any abnormal findings. TTE demonstrated mild aortic valve stenosis (1.3 cm^2 of AVA) with PG across the aortic valve of 33.6 mm Hg with normal wall motion of the left ventricle. MRI of the cervical spine and brain showed findings quite similar to those in Patient 1 (Figs. 2B, D, F and 3B, D, F). Brain, thoracic, and lumbar MRI did not show any dural thickening. CSF examinations demonstrated an elevated protein level (342 mg/dL) without pleocytosis. WAIS-III demonstrated an overall IQ of 75, verbal IQ of 67 and performance IQ of 90.

Both patients underwent dural plasty with laminoplasty to decompress the cervical spinal cord, and the surgery resulted in obvious improvement of spastic gait. Biopsies of the dura mater during the surgery disclosed marked thickening of the collagenous tissue with clear cells containing fine granular materials stained by Alcian-Blue, which is presumably lysosomal inclusions of accumulated glycosaminoglycan in both patients (Fig. 4). Furthermore, both patients initiated enzyme replacement therapy with laronidase, which expected to decrease glycosaminoglycan storage and lead to clinical improvement [6], for MPS-I after surgery.

3. Methods

3.1. Enzymatic assay of IDUA activity

Enzymatic activity of IDUA from peripheral blood leukocytes was measured by fluorometric assay using 4-methylumbelliferyl α-L-iduronide as described previously [7].

3.2. Zygosity testing of the twin

Determination of zygosity was made by PCR-amplified short tandem repeat (STR) analysis [8] with commercially available panels (AmpFLSTR SGM Plus Kit and AmpFLSTR Profiler Kit, Applied Biosystems LLC, Foster City, CA, USA), comprising 15 autosomal, co-dominant, unlinked loci (D3S1358, vWA, FGA, D16S539, D2S1338, TH01, TPOX, CSF1PO, D8S1179, D21S11, D18S51, D5S818, D13S317, D7S820, D19S433), and the gender-determining marker, amelogenin.

3.3. Mutation analysis of the IDUA gene

Genomic DNA was extracted from peripheral blood leukocytes. PCR amplification of each of 14 exons and intron/exon boundaries of *IDUA* was performed as reported in a previous publication [9]. PCR products were sequenced in both the forward and reverse directions on automated DNA sequencing (ABI Prism 3100 Genetic Analyzer) using the BigDye Terminator v3.1 Cycler Sequencing Kit (PE Applied Biosystems, Foster City, CA, USA).

4. Results

4.1. Enzymatic assay of IDUA activity

Both patients showed IDUA activity from peripheral leukocytes <0.9 nmol/mg protein/h (normal range; 29.8–89.8 nmol/mg protein/h), and that of their mother showed 19.9 nmol/mg protein/h.

4.2. Zygosity testing of the twin

All 16 tested loci and marker were identical in our patients, therefore, the patients were estimated to be monozygotic twins with probability of 99.99995% (based on the assumption of an a priori probability at 0.5).

4.3. Mutation analysis of the IDUA gene

Direct sequence from genomic DNA of the twins showed 1 bp insertions, c.252insC (p.P55fxX62), in exon II, and point mutations, c.1209C>A (p.T374N), in exon VIII of *IDUA* in a heterozygous form in the two patients (Fig. 5). These mutations were examined in their mother, who showed only a heterozygous form of the mutant and a wild type sequence for c.252insC (data not shown).

5. Discussion

We report two patients with an attenuated form of MPS-I confirmed by *IDUA* mutations. It was characteristic that these patients showed a quite similar distinctive phenotype: development of cervical myelopathy due to spinal canal stenosis caused by pachymeningeal hypertrophy as an initial and cardinal manifestation at the same age. In

Please cite this article as: Furukawa Y, et al, Cervical pachymeningeal hypertrophy as the initial and cardinal manifestation of mucopolysaccharidosis type I in monozygotic twins with a novel mutation..., J Neurol Sci (2010), doi:10.1016/j.jns.2010.11.022

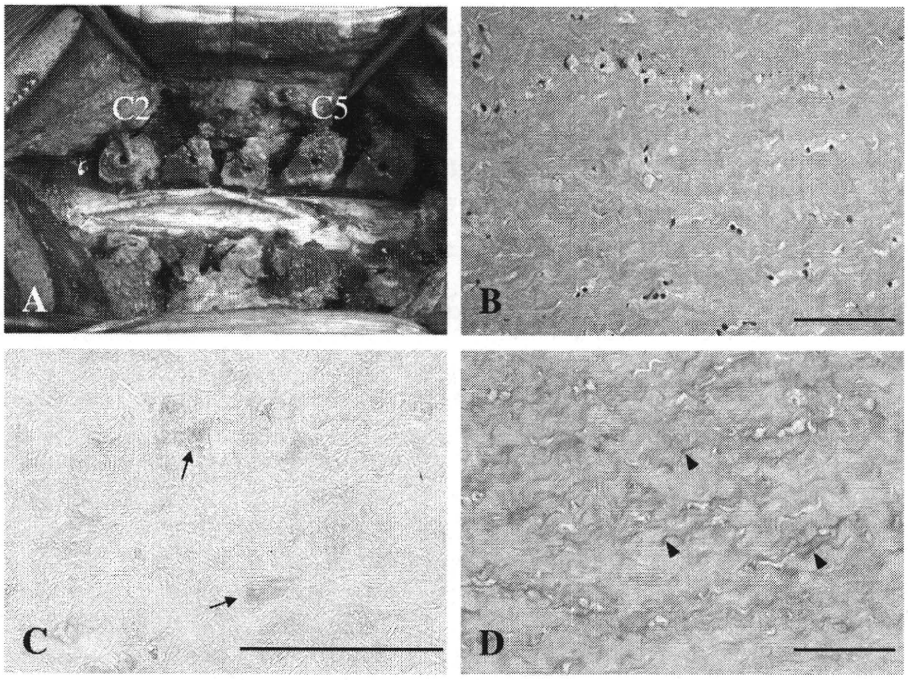

Fig. 4. Surgical and pathological findings of the dura mater of Patient 2. Thickened dura was observed macroscopically (A). Cervical dural biopsy showed clear cells containing fine Alcian-Blue-positive granular materials, which is presumably indicating lysosomal deposit of glycosaminoglycan, within the cytoplasm (arrows), and Periodic acid-Schiff (PAS)-positive deposits between collagenous connective tissue (arrow heads) (B–D) (B: Hematoxylin–eosin stain, C: Alcian-Blue stain, D: PAS stain, scale bar indicates 100 μm).

addition, our patients are short compared with their same generation of Japanese male, and have a history of umbilical and inguinal hernia, mild cardiac valve abnormality, dysostosis multiplex and joint contracture (in Patient 2 only), which are likely MPS-I-related manifestations. Importantly, genetic analyses demonstrated that our patients were monozygotic twins showing the identical mutations of *IDUA*, c.252insC (p.P55fs62X) and c.1209C>A (p.T374N). Although we could not perform *IDUA* analysis of the father, the mother showed only c.252insC mutation. Therefore, the c.1209C>A mutation was inferred to have been inherited from their father, and the patients would have compound heterozygous mutations.

MPS-I has been historically classified into three phenotypes, severe (Hurler), attenuated (Scheie), and intermediate (Hurler/Scheie); however, the clinical spectrum is variable from severe to mild [10]. The clinical features of our patients related to MPS-I are generally mild, and age at diagnosis is relatively late, therefore, we consider our patient as having attenuated form of MPS-I. Our patients each had a history of inguinal and umbilical hernia in early childhood and cervical myelopathy developed two decades after surgical treatment of hernias. This time course of our patients appears to fit the natural history of attenuated form of MPS-I [11]. Cardiac valve abnormalities, joint contracture, corneal clouding, carpal tunnel syndrome, and hernia were reported to be the five most prevalent features of attenuated form of MPS-I [11]. Although our patients each had some features of attenuated MPS-I, they showed no corneal clouding, carpal tunnel syndrome with no or very

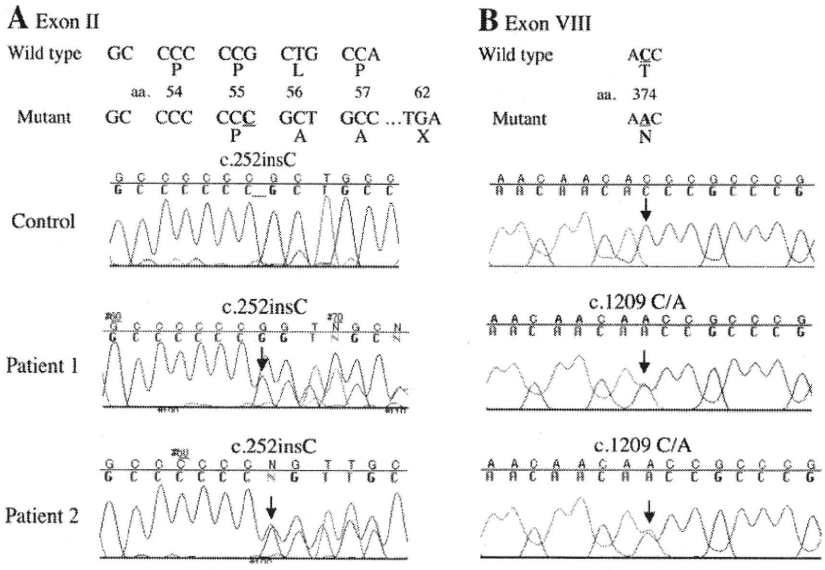

Fig. 5. Direct sequencing of *IDUA* showed 1 bp insertions, c.252insC (p.P55fs62X) (arrows), in exon II (A), and point mutations, c.1209C to A (p.T374N) (arrows), in exon VIII (B) in Patients 1 and 2.

Please cite this article as: Furukawa Y, et al, Cervical pachymeningeal hypertrophy as the initial and cardinal manifestation of mucopolysaccharidosis type I in monozygotic twins with a novel mutation..., J Neurol Sci (2010), doi:10.1016/j.jns.2010.11.022

mild joint contracture. It is remarkable that cervical myelopathy due to pachymeningeal hypertrophy is the opportunity of the diagnosis of MPS-I in our patients. Cervical pachymeningeal hypertrophy has been reported during the clinical course in some cases of MPS-I [4,5]; however, there have been no reports of cervical myelopathy as an initial and cardinal symptom of MPS-I. Meningeal hypertrophy or hypertrophic pachymeningitis may occur in association with several underlying disease such as infection, autoimmune inflammatory disorders or malignancies [12]. MPS-I should be included in the differential diagnosis of pachymeningeal hypertrophy even if other features of MPS-I are absent or trivial.

Over a hundred *IDUA* mutations have been reported in MPS-I; some mutations may be associated with the severity of the disease [2]. Generally, insertion mutations cause frameshift preventing production of the functional enzyme, whereas missense mutations may allow some residual enzymatic activity [1]. In our patients with mutations of c.252insC (p.P55fs62X) and c.1209C>A (p.T374N), it is conceivable that the product of the allele with the c.1209C>A mutation may allow some enzymatic activity, contributing to the attenuated phenotype of MPS-I in our patients.

Our two patients demonstrated quite similar clinical manifestations. Several common mutations of *IDUA* have been reported to be mild or severe, such that the presence of two severe mutations in a patient predicts a severe phenotype, while the presence of at least one mild mutation in a patient predicts an attenuated phenotype [2]. MPS-I patients who have the identical genotype would generally show the same disease severity, for example, homozygosity or compound heterozygosity for the severe mutations, W402X and Q70X (i.e. W402X/W402X, Q70X/Q70X, and W402X/Q70), predicts a severe phenotype, whereas patients with at least one mild R89Q mutation are predicted to have an attenuated phenotype [2]. However, some mutations are known to show the variable severity of the disease even if the patients had identical mutations of *IDUA* [2]. Interestingly, patients with homozygote of P533R missense mutation were reported to be associated with various forms of the disease including both the attenuated [13] and severe [14] forms, suggesting that the disease phenotypes would not be determined only by the genotypes of *IDUA*, but would also be influenced by other genetic or environmental factors [15]. Our patients were monozygotic twins with a quite similar, unique phenotype, suggesting that genetic factors not only *IDUA* mutation but also genes other than *IDUA* may play major roles in determining the phenotypes of MPS-I. Further case studies are needed to clarify the factors that influence the phenotype of MPS-I.

Acknowledgements

The authors thank Dr. M. Okada (Department of Clinical Laboratory Medicine, National Center for Child Health and Development, Tokyo, Japan) for advice on gene analysis, and Ms. Y. Kakuta (Department of Neurology and Neurobiology of Aging, Kanazawa University Graduate School of Medical Science, Kanazawa, Japan) for technical support for pathologic study.

References

[1] Scott HS, Bunge S, Gal A, Clarke LA, Morris CP, Hopwood JJ. Molecular genetics of mucopolysaccharidosis type I: diagnostic, clinical, and biological implications. Hum Mutat 1995;6:288–302.
[2] Terlato NJ, Cox GF. Can mucopolysaccharidosis type I disease severity be predicted based on a patient's genotype? A comprehensive review of the literature. Genet Med 2003;5:286–94.
[3] Pastores GM, Arn P, Beck M, Clarke JT, Guffon N, Kaplan P, et al. The MPS I registry: design, methodology, and early findings of a global disease registry for monitoring patients with Mucopolysaccharidosis Type I. Mol Genet Metab 2007;91:37–47.
[4] Khan SA, Sehat K, Calthorpe D. Cervical cord compression in an elderly patient with Hurler's syndrome: a case report. Spine 2003;28:E313–5.
[5] Munoz-Rojas MV, Vieira T, Costa R, Fagondes S, John A, Jardim LB, et al. Intrathecal enzyme replacement therapy in a patient with mucopolysaccharidosis type I and symptomatic spinal cord compression. Am J Med Genet A 2008;146A:2538–44.
[6] Clarke LA, Wraith JE, Beck M, Kolodny EH, Pastores GM, Muenzer J, et al. Long-term efficacy and safety of laronidase in the treatment of mucopolysaccharidosis I. Pediatrics 2009;123:229–40.
[7] Hopwood JJ, Muller V, Smithson A, Baggett N. A fluorometric assay using 4-methylumbelliferyl α-L-iduronide for the estimation of α-L-iduronidase activity and the detection of Hurler and Scheie syndromes. Clin Chim Acta 1979;92:257–65.
[8] Yang MJ, Tzeng CH, Tseng JY, Huang CY. Determination of twin zygosity using a commercially available STR analysis of 15 unlinked loci and the gender-determining marker amelogenin – a preliminary report. Hum Reprod 2006;21:2175–9.
[9] Scott HS, Litjens T, Nelson PV, Thompson PR, Brooks DA, Hopwood JJ, et al. Identification of mutation in the α-L-iduronidase gene that cause Hurler and Scheie syndromes. Am J Hum Genet 1993;53:973–86.
[10] Neufeld EF, Muenzer J. The mucopolysaccharidosis. In: Scriver CR, Beaudet AL, Sly WS, Valle D, Childs B, Kinzler KW, Vogelstein B, editors. The metabolic and molecular basis of inherited disease. New York: McGraw-Hill; 2001. p. 3421–52.
[11] Thomas JA, Beck M, Clarke JT, Cox GF. Childhood onset of Scheie syndrome, the attenuated form of mucopolysaccharidosis I. J Inherit Metab Dis 2010;33:421–7.
[12] Kupersmith MJ, Martin V, Heller G, Shah A, Mitnick. Idiopathic hypertrophic pachymeningitis. Neurology 2004;62:686–94.
[13] Gatti R, DiNatale P, Villani GR, Filocamo M, Muller V, Guo XH, et al. Mutations among Italian mucopolysaccharidosis type I patients. J Inherit Metab Dis 1997;20:803–6.
[14] Alif N, Hess K, Straczek J, Sebbar S, N'Bou A, Nabet P, et al. Mucopolysaccharidosis type I: characterization of a common mutation that causes Hurler syndrome in Moroccan subjects. Ann Hum Genet 1999;63:9–16.
[15] Clarke LA, Nelson PV, Warrington CL, Morris CP, Hopwood JJ, Scott HS. Mutation analysis of 19 North American mucopolysaccharidosis type I patients: identification of two additional frequent mutations. Hum Mutat 1994;3:275–82.

Please cite this article as: Furukawa Y, et al, Cervical pachymeningeal hypertrophy as the initial and cardinal manifestation of mucopolysaccharidosis type I in monozygotic twins with a novel mutation..., J Neurol Sci (2010), doi:10.1016/j.jns.2010.11.022

4．ライソゾーム病の診断

奥山　虎之
Okuyama　Torayuki

国立成育医療センター 臨床検査部 部長

Summary　ライソゾーム病の診断のプロセスについて，おもにムコ多糖症を中心に説明した。ライソゾーム病の診断は，「蓄積物質の同定」，「ライソゾーム酵素の活性測定」，「遺伝子変異の同定」を有機的に組み合わせて行われる。酵素補充療法などの治療法が開発されたことから早期診断の意義が高まり，新生児マススクリーニングへの導入も検討されている。

はじめに

ライソゾーム病は，ライソゾーム酵素の先天的欠損によりライソゾーム内に分解できない脂質や糖質が過剰蓄積するために，複数の臓器の障害が進行性に現れる単一遺伝子病である。診断のはじめのステップは，特徴的な臨床症状や経過からライソゾーム病を疑うことである。特定の疾患あるいは疾患群が疑えると判断された場合に確定診断へと進む。確定診断には「蓄積物質の同定」，「ライソゾーム酵素の活性測定」，「遺伝子変異の同定」が用いられる。本稿では，比較的頻度が高く系統的な診断プロセスが確立しているムコ多糖症について詳しく述べる。

1．ムコ多糖症について

ムコ多糖は体の主要な構成成分のひとつである。ムコ多糖はライソゾームに局在する約10種類の酵素によって段階的に分解される[1]。酵素のひとつが欠損していると分解が途中でとまり，高分子化合物がライソゾーム内に過剰蓄積し，細胞障害の原因となる。ムコ多糖症は臨床症状と欠損酵素の違いにより，7つの病型に分類される（**表1**）。遺伝形式については，ムコ多糖症Ⅱ型がX連鎖劣性遺伝病で原則として男児にのみ発症するが，その他の疾患は常染色体劣性遺伝病であり，罹患者の性差はない。

2．尿中ムコ多糖の分析

主なムコ多糖には，デルマタン硫酸（DS），ヘパラン硫酸（HS），ケラタン硫酸（KS）などがある。ムコ多糖症では尿中にムコ多糖が過剰排泄される。ムコ多糖を分解する酵素は，上記の3つの物質の1種類あるいは2種類の分解に関与する。たとえば，ムコ多糖症Ⅰ型の欠損酵素であるα-L-イズロニダーゼとムコ多糖症Ⅱ型の欠損酵素L-

表1　ムコ多糖症の病型分類

病型（略号）		欠損酵素	蓄積物質・尿中異常ムコ多糖	遺伝形式
Hurler	(MPS Ⅰ H)	α-L-Iduronidase	デルマタン硫酸 ヘパラン硫酸	常染色体性劣性遺伝
Hurler/Scheie	(MPS Ⅰ H/S)			
Scheie	(MPS Ⅰ S)			
Hunter, severe	(MPS Ⅱ, severe or attenuated)	Iduronate sulfatase	デルマタン硫酸 ヘパラン硫酸	X連鎖性劣性遺伝
Hunter, intermediate	(MPS Ⅱ, intermediate)			
Hunter, mild	(MPS Ⅱ, mild)			
Sanfilippo A	(MPS Ⅲ A)	Heparan N-sulfatase	ヘパラン硫酸	常染色体性劣性遺伝
Sanfilippo B	(MPS Ⅲ B)	α-N-Acetylglucosaminidase		
Sanfilippo C	(MPS Ⅲ C)	Acetyl CoA：α-glucosaminide acetyltransferase		
Sanfilippo D	(MPS Ⅲ D)	N-Acetylglucosamine 6-sulfatase		
Morquio A	(MPS Ⅳ A)	Galactose 6-sulfatase	ケラタン硫酸	常染色体性劣性遺伝
Morquio B	(MPS Ⅳ B)	β-Galactosidase		
Maroteaux-Lamy	(MPS Ⅵ)	N-Acetylgalactosamine 4-sulfatase (arylsulfatae B)	デルマタン硫酸	常染色体性劣性遺伝
Sly	(MPS Ⅶ)	β-Glucuronidase	デルマタン硫酸 ヘパラン硫酸 コンドロイチン硫酸A，C	常染色体性劣性遺伝

ムコ多糖症の病型別の欠損酵素，蓄積物質，遺伝形式を示す。病型により，蓄積するムコ多糖の種類が異なる。

（筆者作成）

イズロネートスルファターゼは，DSとHSの両方の分解に必要であるので，この2疾患ではDSとHSが同時に蓄積することになる。一方，ムコ多糖症Ⅵ型の欠損酵素であるアリルスルファターゼBは，DSの分解には関与するが，HSの分解には関与しないので，DSの蓄積はあるがHSは蓄積しない。このように，尿中のムコ多糖の蓄積パターンを調べることにより，ある程度の病型予測ができる。

3．酵素活性測定

尿中ムコ多糖分析から病型がある程度絞り込まれた場合，特定の疾患の酵素活性を測定することにより診断を確定できる。検体としては，血液中の白血球を用いる。酵素活性測定には，人工基質を用いて，4メチルウンベリフェロンの蛍光発色の強度を定量することが一般的である。

DS（デルマタン硫酸）　HS（ヘパラン硫酸）　KS（ケラタン硫酸）

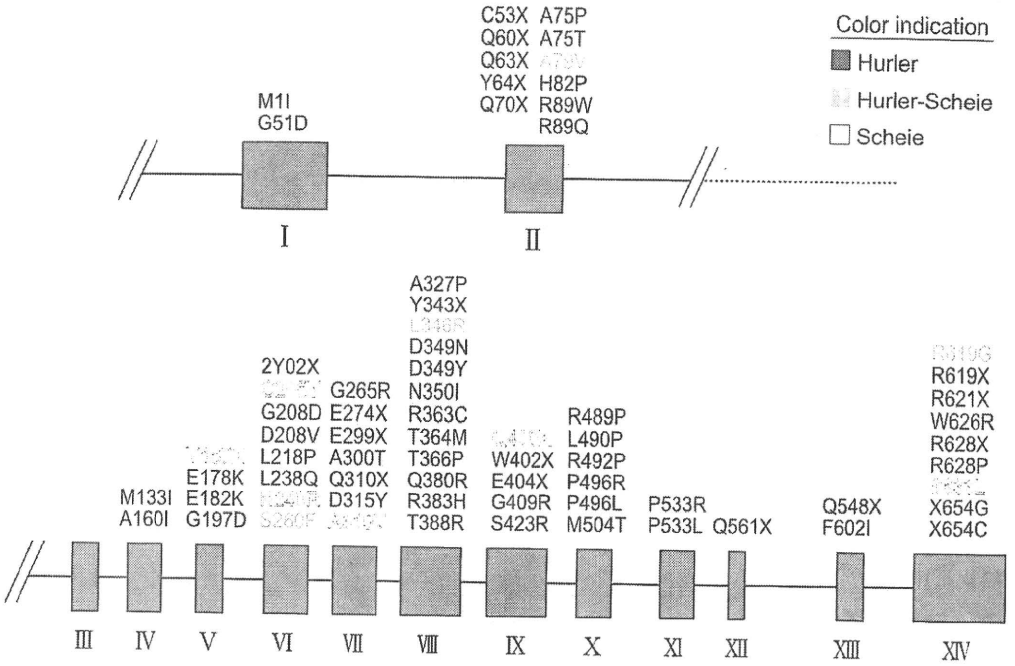

図1　ムコ多糖症Ⅰ型の遺伝子変異

図はムコ多糖症Ⅰ型のこれまでに報告された遺伝子変異のなかで，ミスセンス変異とナンセンス変異だけを示している。変異は多彩であり，ホットスポットはない。（筆者作成）

4．遺伝子解析

ムコ多糖症の原因となるライソゾーム酵素をコードする遺伝子はすべて解明されている。したがって，白血球細胞のDNAなどを用いることにより，遺伝子変異を見出し診断に結びつけることができる。遺伝子解析には以下のような問題点がある。

1）遺伝子変異のホットスポットがないので，症例ごとに遺伝子全体を解析する必要があり，時間，労力，コストがかかる。

2）遺伝子変異には，ミスセンス変異，ナンセンス変異，スプライシング異常などの比較的微細な異常から，遺伝子の組み換えや広範囲な欠失のような大きな異常まで多種多様な異常が存在する（図1）。

3）アミノ酸がひとつだけ置換するような変異（ミスセンス変異）の場合，すでに報告がある変異であれば疾患との関連は強いとされるが，これまでに報告されていない変異の場合，まれな多型の可能性も否定できないので注意を要する。

ムコ多糖症は，原則的には酵素活性の測定により確定診断される。遺伝子解析は診断に必須ではない。しかし，ムコ多糖症Ⅱ型の保因者診断を正確に行うためには，遺伝子解析は不可欠である。

5．出生前診断について

ムコ多糖症は難治性の疾患である。しかし，Ⅰ型，Ⅱ型，Ⅵ型では酵素補充療法が開発されているが，中枢神経症状に対する効果は期待できない。また，その他の病型，特に中枢神経症状が強く出るⅢ型については，有効な治療手段は今のと

ころ全く存在しない。そのため，疾患患者を持つ家族では，発端者の次の子に対して出生前診断を希望する家族も少なくない。出生前診断は，絨毛細胞や羊水細胞の酵素活性を測定することで可能である。また，予め発端者の遺伝子解析の原因となる変異が確定している家族においては，絨毛細胞や羊水細胞を用いた遺伝子解析が有用である。なお，出生前診断を行う場合は，疾患の診療経験が豊富な専門医による遺伝カウンセリングを検査前に行い，検査の限界やメリット，デメリットなどを検査を受ける人に十分に理解してもらう必要がある。

6．新生児スクリーニング（NBS）について

ほとんどのライソゾーム病は，新生児期には目立った症状がない。ムコ多糖などの高分子物質が蓄積し種々の臓器障害を呈するまでには，時間がかかるからである。ムコ多糖症の場合，1～2歳で診断される場合もあるが，5～6歳まで診断されずにいることも多い。酵素補充療法や造血幹細胞移植の効果を考えると，早期にまだ目立った症状が出現する以前に治療を始めることが望ましい。たとえば，ムコ多糖症の骨病変については，症状が明らかになった後では，どのような治療をしても十分な効果は得られない。これに対して，発症前に診断を確定し治療を開始すると，骨病変などの進展に対する予防的な効果が期待できる。そのため，少なくとも治療が可能となった疾患については，新生児マススクリーニングを導入すべきという意見がある。しかし，ライソゾーム病の多くが中枢神経障害があり，現在可能な治療のいずれもが十分な治療効果がないことを考慮すると，新生児マススクリーニングの対象疾患とするには，倫理的な配慮も必要になろう[2]。

文　献

1) 折居忠夫：ムコ多糖症の診断と治療．SRL宝函 27：117-126, 2003
2) 奥山虎之，高柳正樹，遠藤文夫：保険収載されたライソゾーム病5疾患の遺伝病学的検査および遺伝カウンセリングの実施に関するガイドライン．日本小児科学会雑誌 113：789-790, 2009